

## Short Contribution

# Direct Current Measurements off Sanriku, East of Japan

SACHIIHIKO ITOH\* and TAKASHIGE SUGIMOTO

Ocean Research Institute, University of Tokyo, Minamidai, Nakano-ku, Tokyo 164-8639, Japan

(Received 25 September 2001; in revised form 4 April 2002; accepted 4 April 2002)

**One year records of four current meters moored at two sites off Sanriku (39°26' N, 142°45' E and 143°E) have been analyzed. Mean currents flowed southward to southwestward with velocity 2.5–7.8 cm s<sup>-1</sup>. The geostrophic velocity appeared to be surface-intensified, and the flows at 500 m depth have a relationship with the 100 m depth temperature distribution, suggesting the influence of the upper layer flows. At a depth of 1500 m and 2500 m, southward to southwestward flows are thought to be a part of the current flowing southward on the western flank of the Japan Trench.**

Keywords:

· Direct current measurement,  
· Kuroshio-Oyashio Transition region.

## 1. Introduction

The Kuroshio-Oyashio Transition region (KOTR), defined here as the confluence of the Kuroshio and the Oyashio current system, exhibits many variable features, such as eddies, rings, and streamers. The intrinsic mixing and turbulence characteristics often lead its being referred to as “the Mixed Water Region” or “the Perturbed Area”. Kawai (1972) presented a systematic description of this area, mainly of the upper layer. There have been many studies related to dynamical processes such as the northward spread of the Kuroshio Extension (Sainz-Trápaga and Sugimoto, 1998), the structure and movement of warm-core rings (Kitano, 1975; Yasuda *et al.*, 1992; Mishra and Sugimoto, 2000; Itoh and Sugimoto, 2001b), southward penetration of the Oyashio water system (Hanawa, 1995), the ring-ring interaction (Yasuda, 1995), and ring-Oyashio interaction (Itoh and Sugimoto, 2001a).

In addition to these dynamical features in the upper layer, recent studies have reported the intrusion of the Oyashio water through the intermediate layer, and its has been suggested that this becomes North Pacific Intermediate Water (NPIW), characterized by a salinity minimum (Yasuda *et al.*, 1996; Yasuda, 1997; Okuda *et al.*, 2001; Shimizu *et al.*, 2001). The description of the flow patterns has not been completed, however. The existence of the intermediate intrusion was mainly inferred not from directly measured flows but from the distribution of the water masses, and thus the dynamical structure of the in-

trusion is still ambiguous. One of our major interests in this paper is to study the relationship between the intermediate intrusion and the upper layer flows.

As for the deep layer, flows are expected to exist in KOTR, since deep currents have been observed flowing along the bottom slope of the Japan Trench off Hokkaido (Kawasaki *et al.*, 1990; Uehara and Miyake, 1999; Owens and Warren, 2001), and off Boso Peninsula (Hallock and Teague, 1996; Fujio *et al.*, 2000). A few observations on the continental slope support this assumption (Inagake, 1996; Mitsuzawa and Holloway, 1998), but these data are still not sufficient to confirm the description of the deep currents in KOTR.

We have conducted direct current measurements in an attempt to understand the flow field in the intermediate and the deep layers in the western flank of Japan Trench as part of KOTR. Current meter data and collaborative CTD data are analyzed, and the statistics of the flows, water properties, and the relation to the upper layer flows are discussed.

## 2. Data and Methods

The mooring systems were deployed at 39°26' N, 142°45' E (St. A), and 39°26' N, 143°22' E (St. B), along the western slope of the Japan Trench (Fig. 1). At St. A, two current meters were set at 500 m (CM1) and 1500 m (CM2) depth. At St. B three were at 500 m (CM3), 1500 m (CM4), and 2500 m (CM5) depth. However, as CM3 did not work properly, our analyses exclude the data of CM3. In this text, we use the words CM1, CM2, CM4, and CM5 to denote both the current meters themselves and their location. The current meters used were of types Aanderaa RCM9 for CM1 and Aanderaa RCM8 for CM2,

\* Corresponding author. E-mail: itohsach@ori.u-tokyo.ac.jp

Table 1. Station locations, depths and periods of current observations.

Data	Station (Location)	Depth [m]	Period
CM1	A (39°26' N, 142°45' E)	500	15 Apr. 00–11 Apr. 01
CM2	A (39°26' N, 142°45' E)	1500	15 Apr. 00–11 Feb. 01
CM4	B (39°26' N, 143°22' E)	1500	15 Apr. 00–11 Apr. 01
CM5	B (39°26' N, 143°22' E)	2500	15 Apr. 00–11 Apr. 01

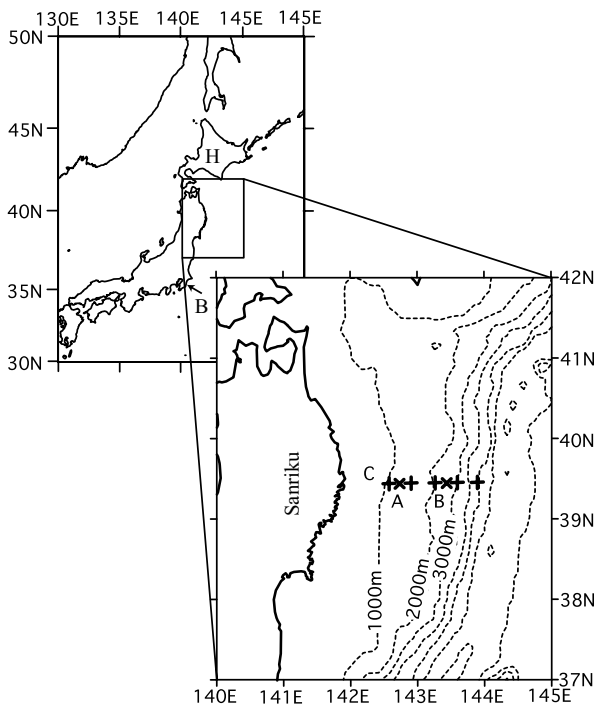


Fig. 1. Geographical location of mooring stations A, B (crosses “x”), CTD stations (pluses “+”), and the line C that intersects these observation sites. Hokkaido and Boso Peninsula are specified in the upper-left panel by the character “H” and “B”.

CM4, and CM5. Current records were obtained from 15 April 2000 to 22 April 2001, except for CM2, which stopped working on at February 2001 (Table 1).

Velocity data obtained at 1 hour intervals are filtered by the 48-hour tide-killer filter, originally designed by Thompson (1983) and developed by Hanawa and Mitsudera (1985) for the adjacent sea of Japan. Filtered data were resampled as daily data. These data were then analyzed to describe the statistical characteristics of the flows. Temperature and salinity were also observed along the line C (Fig. 1) in June 2000 and in April 2001, and geostrophic velocities have been calculated relative to the low-pass filtered flow. Due to the filtering, there is 5-day lag for the data in April 2001.

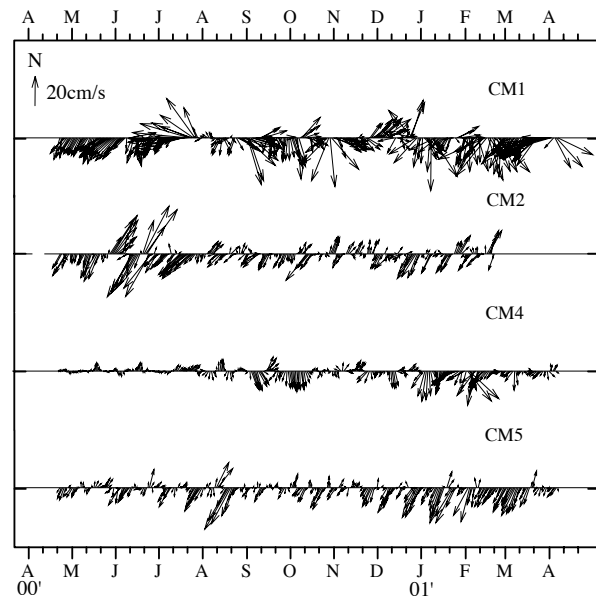


Fig. 2. Time series of the vectors of the low-pass filtered flows at CM1 (39°26' N, 142°45' E; 500 m), CM2 (39°26' N, 142°45' E; 1500 m), CM3 (39°26' N, 143°22' E; 1500 m), and CM4 (39°26' N, 143°22' E; 2500 m).

### 3. Result

#### 3.1 Mean field and statistics

Figure 2 shows the time series of low-pass filtered flows for each station. Arrows indicate daily velocity vectors for the observation periods. Statistics are listed in Table 2, and mean velocity vectors and standard deviation ellipses are presented in Fig. 3. The magnitudes of the mean flows are  $2.5\text{--}7.8\text{ cm s}^{-1}$ , with direction  $186\text{--}217^\circ\text{T}$ , approximately along the local isobaths (Fig. 1). The standard deviations are larger than the mean, but the standard errors are smaller than the mean velocities using the t-test (Table 2, Fig. 3). The standard ellipse for the data of CM2, CM4, and CM5 are clearly flat, i.e., the variabilities are anisotropic, and their major axis orientations are nearly along the isobaths as are those of mean flows. The flatness is not clear, however, and the major axis does not run along the isobaths for CM1.

Table 2. Statistical parameters of the low-pass filtered velocity.  $\bar{V}$  and  $\theta_0$  are the mean magnitude and direction, and  $V_1(V_2)$ ,  $\sigma_1(\sigma_2)$ , and  $\theta_1$  are the major (minor) axis component of the standard deviation, standard error, and the major axis orientation.  $T_1(T_2)$  and  $N_1(N_2)$  are the integral time scale and the effective degrees of freedom of the major (minor) axis component of the flows. The integral (decorrelation) time scales are calculated by summing the normalized autocorrelation function to the first zero crossing, and the effective degrees of freedom are estimated by dividing the record length by the integral time scale.

Data	$\bar{V}$ [cm s <sup>-1</sup> ]	$\theta_0$ [° T]	$V_1$ [cm s <sup>-1</sup> ]	$V_2$ [cm s <sup>-1</sup> ]	$\sigma_1$ [cm s <sup>-1</sup> ]	$\sigma_2$ [cm s <sup>-1</sup> ]	$\theta_1$ [° T]	$T_1$ [days]	$T_2$ [days]	$N_1$	$N_2$
CM1	7.8	196	12.2	9.1	2.3	1.5	80	12.0	9.0	29	39
CM2	3.2	217	10.2	2.2	0.9	0.3	33	2.6	4.6	117	67
CM4	2.5	186	5.5	3.4	1.0	0.3	14	11.6	3.5	30	99
CM5	4.5	208	7.4	1.4	0.6	0.1	26	2.6	1.3	135	275

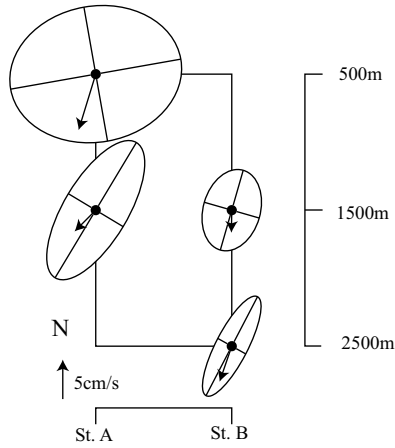


Fig. 3. Mean velocity vectors and standard deviation ellipses of the flows.

### 3.2 Hydrography

Figure 4 shows vertical cross sections of temperature and salinity along line C. The classification of water systems by Hanawa and Mitsudera (1986) distinguishes the Tsugaru Warm Current water system (TW; Temperature  $T$  [°C]  $\geq 5$ ,  $33.7 \leq$  Salinity  $S$  [psu.]  $\leq 34.2$ , and potential density  $[\sigma_\theta] \geq 24.0$ ), the Oyashio water system (OW;  $T$  [°C]  $\leq 7$ ,  $33.0 \leq S$  [psu.]  $\leq 33.7$ , and potential density  $[\sigma_\theta] \leq 26.7$ ), the cold lower-layer water system (CL; not TW and potential density  $[\sigma_\theta] \geq 26.7$ ), and the surface layer water system (SW) (see figure 5 of Hanawa and Mitsudera (1986) for details). In both cases of June (Figs. 4(a), (c), and (e)) and April (Figs. 4(b), (d), and (f)), water masses below 300 m fall on CL, while in the upper layer (shallower than 300 m), TW and OW were seen on the western and eastern sides of the line C, respectively: a TW-OW front was formed and traversed the line C in the upper layer above the current meters. It is noted that the salinity minimum can be found in the layer at 200–300 m depth.

According to the definition by Shimizu *et al.* (2001), the water at CM1 (potential temperature  $\sim 3.5$  [°C],  $S \sim 33.9$  [psu.] potential density  $\sim 26.9$  [ $\sigma_\theta$ ]) corresponds to a 60% mixing ratio of the pure Oyashio water (see their Fig. 2). The waters at CM2, CM4, and CM5 are difficult to characterize due to the insufficient accuracy.

Figure 5 shows the vertical distributions of geostrophic velocity calculated from CTD and the current meter data. At St. A, southward flows are estimated in the upper layer both in June 2000 and April 2001. The velocity is nearly 30 cm s<sup>-1</sup> at the surface and decreases with increasing depth to become northward below 1000 m. In contrast, velocities in June 2000 and April 2001 were lower than 10 cm s<sup>-1</sup> and the directions were opposite at St. B.

## 4. Discussion

### 4.1 Relationship between the observed flows and the upper layer flows

Since the geostrophic flow at St. A was surface-intensified, it is worth investigating the relationship between the observed flows and near-surface temperature fields to discuss the influence of upper layer fluctuations on the current meter data. The 100 m depth temperature is often used to distinguish the upper layer water masses in this region, and the depth is shallower than the salinity minimum layer (Fig. 4) which characterizes the intermediate water. Figure 6 shows three types of horizontal distributions of temperature at 100 m depth (adopted from the 10-day report by Hakodate Marine Observatory, 2000–2001). Current meter stations are sometimes located at a complex confluence (Fig. 6(a)), and at other times at the sharp front (Fig. 6(b)). The water temperature in Fig. 6(c) is more homogeneous than in Figs. 6(a) and (b), but this is mainly due to the wide coverage of the Oyashio water, which is relatively homogeneous in the horizontal direction. Note that the original reports are based on hydrographic data interpolated both in time and space. Warm (cold) water such as Kuroshio (Oyashio) water

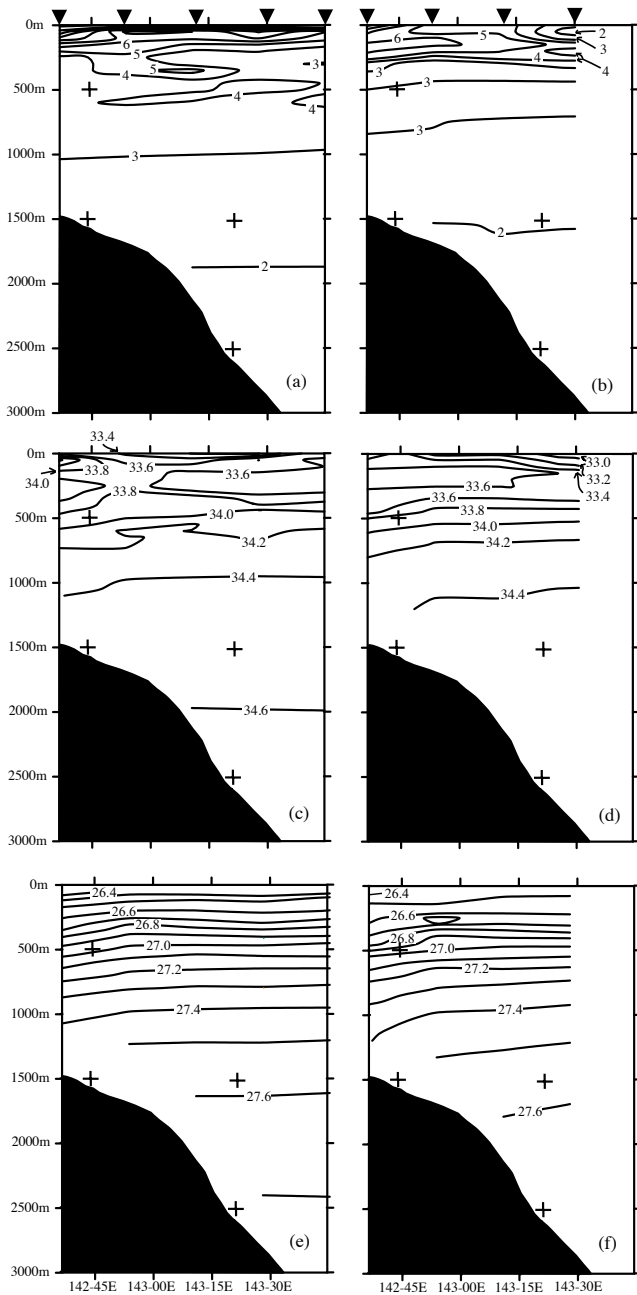


Fig. 4. Temperature [ $^{\circ}\text{C}$ ], salinity [psu.] and potential density [ $\sigma_{\theta}$ ] cross-section along line C ( $39^{\circ}26' \text{N}$ ): (a) temperature at 1 June 2000, (b) temperature at 11 April 2001, (c) salinity at 1 June 2000, (d) salinity at 11 April 2001, (e) potential density at 1 June 2000, and (f) potential density at 11 April 2001. The locations of the current meters are shown with pluses, and CTD stations are indicated by inverted triangles.

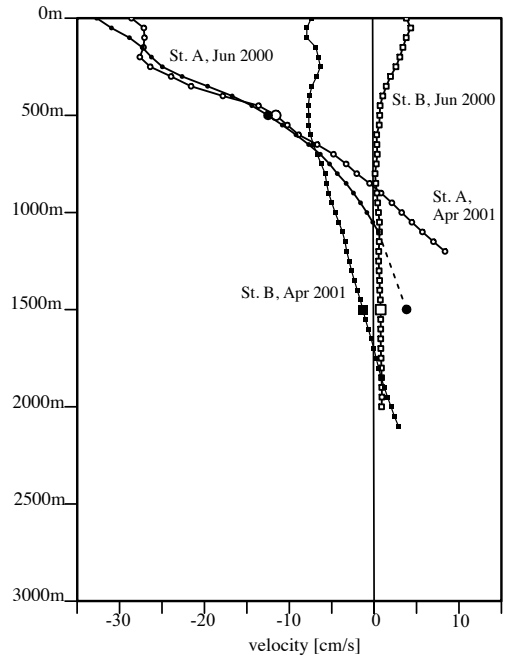


Fig. 5. Vertical distributions of geostrophic velocity normal to line C using the low-pass filtered current meter velocity as references at St. A and St. B. Large marks are the current meter data, and positive values indicate northward velocity. Note that there is a 5-day lag between the data of CTD and current meters CM1, CM4, and CM5 for April 2001 due to the filtering.

generally has high (low) surface dynamic height and flows are anticyclonic (cyclonic) along the isotherms. It is expected that the flow is along the contours with the warmer part to their right. We read the directions of the 10-day data of the temperature contours in an angle interval of  $22.5^{\circ}$  (the 16 points), and compared them with the current meter data. Figure 7 shows the estimated flow directions at St. A and the observed directions of CM1. Even with this rough estimate, the correspondence is good except for the periods of late July–late August, late December, and March. Actually, late July was when St. A was located at the complicated confluence (Fig. 6(a)), and March was when the waters became homogeneous and fronts were difficult to recognize (Fig. 6(c)).

In regard to the other deeper velocity fields at CM2, CM4, and CM5, we cannot detect the relation with upper layer flows like CM1. The flow at CM1 thus might not be correlated with the others. The cross-correlation function of the flows between two vector series  $\mathbf{v}_1(t)$ ,  $\mathbf{v}_2(t)$  is defined as

$$R(r, \phi; \tau) = r e^{i\phi} = \frac{E[\mathbf{v}_1(t)\mathbf{v}_2(t+\tau)]}{\sqrt{E[\mathbf{v}_1(0)]E[\mathbf{v}_2(0)]}}, \quad (1)$$

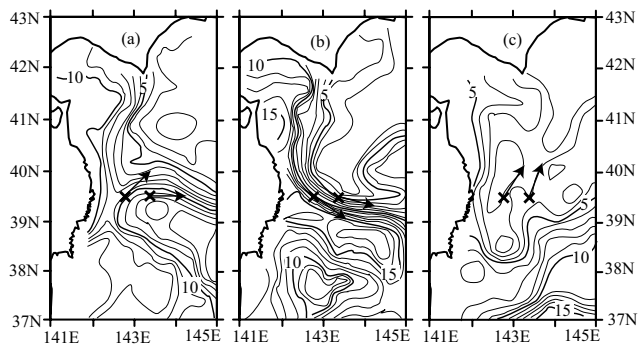


Fig. 6. Horizontal distribution of temperature at 100 m at (a) late July 2000, (b) mid September 2000, and (c) early March 2001 (adopted from Hakodate Marine Observatory, 2000–2001). Crosses (x) indicate the current meter stations, and arrows are estimated flow direction. The contour interval is 1°C.

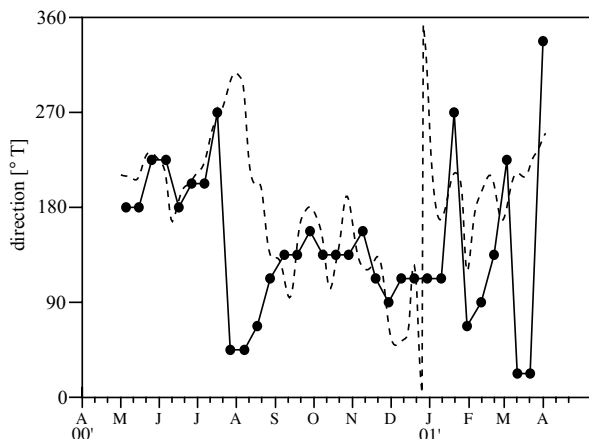


Fig. 7. Time series of current directions in an angle interval of 22.5° (the 16 points) read from the horizontal temperature contours at 100 m depth (solid circles with a solid line), and the smoothed flow directions of CM1 (dashed line). A 10-day Gaussian filter was used for smoothing.

where  $r$ ,  $\phi$ ,  $\tau$  is a magnitude, angle difference, time lag, and  $E[x]$  denotes the ensemble average of  $x$ . The maximum  $r$  for CM1–CM2, in the lag range of –10-day to 10-day, is 0.21 at –3-day lag; the angle difference at –3-day lag is  $-60^\circ$ . The correlation is weak and smaller than the 5% significance level of 0.35 for the equivalent degree of freedom  $N_e = 30$ . The cross-correlations between CM1 and the other currents meters were also not significant.

#### 4.2 Comparison of the observed deep flows with previous studies

The mean flows at CM2, CM4, and CM5 were significantly larger than standard error, hence it is meaning-

ful to compare them with deep currents reported in previous studies. Since our mooring systems are on the western flank of the Japan Trench, we consulted the studies reporting the flows on or above the western flank. Off Hokkaido, mean southwestward flows were observed:  $7.3 \text{ cm s}^{-1}$  at 1710 m (Kawasaki *et al.*, 1990),  $1\text{--}3 \text{ cm s}^{-1}$  at 3000 m (Uehara and Miyake, 1999), and  $0.2\text{--}5.3 \text{ cm s}^{-1}$  at 3000–4000 m (Owens and Warren, 2001). Off Boso Peninsula, mean southward flows were observed:  $1\text{--}2 \text{ cm s}^{-1}$  along the 3000–4000 m slope (Hallock and Teague, 1996),  $2.0\text{--}6.7 \text{ cm s}^{-1}$  at 4200–6300 m. Near the mooring sites in the present study, Inagake (1996) reported  $0.6/1.7 \text{ cm s}^{-1}$  mean southward velocity at  $(38^\circ 16' / 36' \text{ N}, 143^\circ 32' \text{ E})$  at 2500 m depth, and Mitsuzawa and Holloway (1998) reported  $4.0 \text{ cm s}^{-1}$  mean southward velocity at  $(39^\circ 25' \text{ N}, 144^\circ 05' \text{ E})$  at 5800 m depth. The direction of mean flows of CM2, CM4, and CM5 are also southward-southwestward. The magnitudes of the flows depend on observation sites and depth, but those of CM2, CM4, and CM5 are within the observed range. They therefore seem to be parts of the deep current flowing southward on the western flank of the Japan Trench.

#### Acknowledgements

We are grateful to Dr. S. Kimura, H. Nagae, and the members of Division of Fisheries Environmental Oceanography, as well as the officers and the crews of RV Tanseimaru and Hakuohmaru, Ocean Research Institute, the University of Tokyo, for their help in the current meter moorings and the hydrographic observations. We appreciate Dr. I. Yasuda for his comprehensive suggestion, and A. Nagano for his advices on data analysis methods. Thanks are extended to the editor and reviewers for their objective work and constructive comments.

#### References

- Fujio, S., D. Yanagimoto and T. Taira (2000): Deep current structure above the Izu-Ogasawara Trench. *J. Geophys. Res.*, **105**, 6377–6386.
- Hakodate Marine Observatory (2000–2001): Ten-day Marine Report, 220–258.
- Hallock, Z. R. and W. J. Teague (1996): Evidence for a North Pacific deep western boundary current. *J. Geophys. Res.*, **101**, 6617–6624.
- Hanawa, K. (1995): Southward penetration of the Oyashio water system and the wintertime condition of the midlatitude westerlies over the North Pacific. *Bull. Hokkaido Reg. Fish. Res. Lab.*, **59**, 103–120.
- Hanawa, K. and H. Mitsudera (1985): On the constructing daily mean data from oceanic data—Note on dealing with daily mean data. *Bull. Coast. Oceanogr.*, **23**, 79–87 (in Japanese).
- Hanawa, K. and H. Mitsudera (1986): Variation of water system distribution in the Sanriku coastal area. *J. Oceanogr. Soc. Japan*, **42**, 435–446.
- Inagake, D. (1996): Observations of deep current velocities east of Kinka-zan from October 1991 to October 1993. *Tohoku*

- Natl. Fish. Res. Inst.*, **58**, 61–75 (in Japanese with English abstract).
- Itoh, S. and T. Sugimoto (2001a): Dynamics of long-term northward movement of warm-core rings and their effect on fishing ground formation. *Bull. Japan Soc. Fish. Oceanogr.*, **65**, 15–21 (in Japanese with English abstract).
- Itoh, S. and T. Sugimoto (2001b): Numerical experiments on the movements of a warm-core ring with the bottom slope of a western boundary. *J. Geophys. Res.*, **106**, 26,851–26,862.
- Kawai, H. (1972): Hydrography of the Kuroshio Extension. p. 235–352. In *Kuroshio, It's Physical Aspects*, ed. by H. Stommel and K. Yoshida, Chapter 8, University of Tokyo Press.
- Kawasaki, H., T. Kono and T. Sugimoto (1990): Current speed variability of the Oyashio. *Kaiyo Monthly*, **22**, 199–210 (in Japanese).
- Kitano, K. (1975): Some properties of the warm eddies generated in the confluence zone of the Kuroshio and Oyashio currents. *J. Phys. Oceanogr.*, **5**, 245–252.
- Mishra, P. and T. Sugimoto (2000): Formation processes and associated events in the evolution of Kuroshio warm core ring. In *Proceedings of the PORSEC 2000 Goa, India*, **2**, p. 565–570.
- Mitsuzawa, K. and G. Holloway (1998): Characteristics of deep currents along trenches in the northwest Pacific. *J. Geophys. Res.*, **103**, 13,085–13,092.
- Okuda, K., I. Yasuda, Y. Hiroe and Y. Shimizu (2001): Structure of subsurface intrusion of the Oyashio water into the Kuroshio Extension and formation process of the North Pacific Intermediate Water. *J. Oceanogr.*, **57**, 121–140.
- Owens, W. B. and B. A. Warren (2001): Deep circulation in the northwest corner of the Pacific Ocean. *Deep-Sea Res. I*, **48**, 959–993.
- Sainz-Trápaga, S. and T. Sugimoto (1998): Spreading of warm water from the Kuroshio Extension into the perturbed area. *J. Oceanogr.*, **54**, 257–272.
- Shimizu, Y., I. Yasuda and S.-I. Ito (2001): Distribution and circulation of the coastal Oyashio intrusion. *J. Phys. Oceanogr.*, **31**, 1561–1578.
- Thompson, R. O. R. Y. (1983): Low-pass filters to suppress inertial and tidal frequencies. *J. Phys. Oceanogr.*, **13**, 1077–1083.
- Uehara, K. and H. Miyake (1999): Deep flows on the slope inshore of the Kuril-Kamchatka trench southeast off cape Erimo, Hokkaido. *J. Oceanogr.*, **55**, 559–574.
- Yasuda, I. (1995): Geostrophic vortex merger and streamer development in the ocean with special reference to the merger of Kuroshio warm core rings. *J. Phys. Oceanogr.*, **25**, 980–996.
- Yasuda, I. (1997): The origin of North Pacific Intermediate Water. *J. Geophys. Res.*, **102**, 893–909.
- Yasuda, I., K. Okuda and M. Hirai (1992): Evolution of a Kuroshio warm-core ring—variability of the hydrographic structure. *Deep-Sea Res.*, **39**, S131–S161.
- Yasuda, I., K. Okuda and Y. Shimizu (1996): Distribution and modification of North Pacific Intermediate Water in the Kuroshio-Oyashio interfrontal zone. *J. Phys. Oceanogr.*, **26**, 448–465.